



Title	Preparation of platinized strontium titanate covered with hollow silica and its activity for overall water splitting in a novel phase-boundary photocatalytic system
Author(s)	IKEDA, Shigeru; HIRAO, Ko; ISHINO, Satoru; MATSUMURA, Michio; OHTANI, Bunsho
Citation	Catalysis Today, 117(1-3), 343-349 https://doi.org/10.1016/j.cattod.2006.05.037
Issue Date	2006-09-30
Doc URL	http://hdl.handle.net/2115/48671
Type	article (author version)
File Information	CatalToday117_343.pdf



[Instructions for use](#)

Preparation of platinumized strontium titanate covered with hollow silica and its activity for overall water splitting in a novel phase-boundary photocatalytic system

Shigeru IKEDA,^{a,b*} Ko HIRAO,^a Satoru ISHINO,^a Michio MATSUMURA,^a and Bunsho OHTANI^c

^a*Research Center for Solar Energy Chemistry, Osaka University, 1-3 Machikaneyama, Toyonaka, Osaka 560-8531, Japan*

^b*“Conversion and Control by Advanced Chemistry”, PRESTO, Japan Science and Technology Agency (JST), Japan*

^c*Catalysis Research Center, Hokkaido University, Sapporo 001-0021, Japan*

Abstract

Platinum-loaded strontium titanate (Pt-SrTiO₃) (core) –silica (shell) powder was prepared by double-layer winding of a carbon and a silica layer on Pt-SrTiO₃ followed by heat treatment to remove the carbon layer. Scanning electron microscope (SEM) observation and analyses of the BET surface area suggested that the powder has a void space between Pt-SrTiO₃ (core) and silica (shell). When the surface of the powder was partially modified with a fluoroalkylsilylation agent, thus-obtained material assembled at a gas-water interface and acted as a photocatalyst for overall water splitting to produce hydrogen (H₂) and oxygen (O₂). Probably due to the suppression of a backward reaction, production of water from H₂ and O₂, on the platinum, the overall efficiency of this system was higher than that of the conventional suspension system. Moreover, while the Pt-SrTiO₃ powders directly covered with fluoroalkylethylsilyl groups showed low photostability, i.e., prolonged irradiation precipitated some of the surface-modified

particles in water owing to photocatalytic decomposition of surface fluoroalkylethylsilyl groups, this material could retain its location at the phase boundary.

Keywords

photocatalytic water splitting; platinum loaded photocatalysts; gas-water interface; silica coating; amphiphilicity; core-shell structure; void space; backward reaction; photostability.

*Corresponding author.

Tel: +81-6-6850-6696; fax; +81-6-6850-6699

E-mail address: sikeda@chem.es.osaka-u.ac.jp

1. Introduction

Overall water splitting is one of the most exciting reactions in photocatalysis since it has potential application to direct production of H₂ for clean energy using photon energy [1,2]. A considerable number of solid photocatalysts for overall water splitting have been discovered in extensive research [3-12]. In most cases, photocatalysts utilized for the reaction are formed by the combination of transition metal oxides and promoters: the former has the function of generating photoexcited electrons and holes, whereas the latter, usually fine metal or metal oxide particles dispersed on metal oxides, acts as a reduction catalyst of water into H₂.

Among reduction catalysts, platinum (Pt) is the best metal for H₂ liberation because of its smallest overpotential of water reduction. Indeed, many studies have shown that Pt-loaded photocatalysts show efficient activity for H₂ liberation from

aqueous suspensions containing sacrificial reagents such as alcohols [13-16]. However, the overall water splitting reaction, stoichiometric photocatalytic decomposition of water into H₂ and O₂, scarcely proceeds on Pt-loaded photocatalysts under ambient conditions because of the high activity of Pt for a backward reaction, i.e., production of water from H₂ and O₂.

In the past decade, some researchers have succeeded in overcoming the problem of photocatalytic overall water splitting on Pt-loaded photocatalysts by improving reaction conditions and photocatalysts [17-19]. Sato et al. showed in their pioneering work on Pt-loaded photocatalytic systems that Pt-loaded TiO₂ (Pt-TiO₂) coated with NaOH could decompose water vapor [17]. Tabata et al. reported that the overall water splitting of pure water can be achieved by just changing the mode of photoirradiation; an aqueous Pt-TiO₂ suspension was irradiated from the top of a reaction cell but not from the bottom or side of the cell [18]. They claimed that the further the photoirradiated particles are from the water level, the faster is the backward reaction of H₂ and O₂ suppressing the overall rate, and top-irradiation reduces the distance, resulting in higher efficiency. From their findings, the appropriate condition for overall water splitting on Pt-loaded photocatalysts seems to be that photocatalysts presented at the gas-water interface.

Recently, we have found a facile method for assembling oxide materials at oil-water and gas-water interfaces by partial modification of external surfaces of particles with an alkylsilane agent [20-25]. One of the most noticeable features of these amphiphilic materials is that the assembled particles loaded with small amounts of titanium(IV) oxide acted as an efficient catalyst for oxidation of several hydrophobic alkenes and alcohols with aqueous hydrogen peroxide without mechanical agitation [20-23]. The reaction system is thus named phase-boundary catalysis.

We have also proposed the possibility of application of a phase-boundary catalytic system to liquid-liquid and gas-liquid dual-phase photocatalytic reactions [26]. For

these systems, it was confirmed that alkylsilane agents should be loaded indirectly to the surface of photocatalysts in order to inhibit photocatalytic decomposition of surface-covered alkylsilyl groups: the photostability was considerably improved when commercially available TiO₂ particles coated with porous silica (SiO₂) [27] were employed as a starting material and the surface of SiO₂ was modified with an alkylsilane agent.

On the basis of these facts and findings, our research interest is focused on development of a system for efficient photocatalytic overall splitting using Pt-loaded photocatalysts assembled at the gas-water interface. In this study, we prepared Pt-loaded SrTiO₃ photocatalysts covered with hollow silica, made their surfaces amphiphilic so that the particles would assemble at the gas-water interface, and used them for the phase-boundary photocatalytic water splitting.

2. Experimental

2.1 Preparation of Pt-loaded SrTiO₃

Platinum-loaded SrTiO₃ (Pt-SrTiO₃) was prepared by a photodeposition method [15]. Typically, 1 g of SrTiO₃ (Fuji Titanium Industry) suspended in an aqueous solution (150 cm³) containing methanol (10 vol%) and 5 μmol of chloroplatinic acid (H₂PtCl₆·6H₂O) was photoirradiated (> 290 nm, see below) in argon (Ar) for 3 h with magnetic stirring (ca. 1000 rpm) and this was followed by washing with water several times and drying to achieve 0.1 wt% loading of Pt.

2.2 Incorporation of Pt-SrTiO₃ into hollow silica

Incorporation of Pt-SrTiO₃ into hollow silica was conducted by successive coating of Pt-SrTiO₃ with a carbon layer and a silica layer followed by heat treatment to remove the carbon layer. First, a carbon layer was coated on Pt-SrTiO₃ by using a procedure similar to that used for carbon-coatings of silver and gold nanoparticles [28]. To an aqueous solution (80 cm³) containing 40 mmol of glucose, 0.5 g of Pt-SrTiO₃ was added. The suspension was placed in a Teflon-sealed autoclave and maintained at 453 K for 3 h. The brown powder was isolated by filtration, washed with water and ethanol, and heated at 773 K under evacuation for 2 h. Then 0.3 g of carbon-coated Pt-SrTiO₃ (c/Pt-SrTiO₃) thus-obtained was suspended in a mixed solution of ethanol (60 cm³) and water (5 cm³) containing 150 μmol of aminopropyltriethoxysilane (APS). After stirring the suspension for 24 h at room temperature, 500 μmol of tetraethyl orthosilicate (TEOS) was added and the suspension was further stirred for 24 h. The solid part was collected by filtration, washed with water several times, and heated at 783 K under vacuum to yield silica-coated c/Pt-SrTiO₃ (si/c/Pt-SrTiO₃). Finally, the carbon component in the si/c/Pt-SrTiO₃ powder was removed by heating the sample at 873 K for 3 h in air to obtain Pt-SrTiO₃ incorporated into the silica layer (*p*-si/Pt-SrTiO₃). As a reference, Pt-SrTiO₃ coated with silica (*n*-si/Pt-SrTiO₃) was prepared without coating with carbon in the first step of the procedure for preparing *p*-si/Pt-SrTiO₃.

2.3 Modification of particle surface with a fluoroalkylethylsilylation agent

Functionalization of external surfaces of Pt-SrTiO₃, and *p*-si/Pt-SrTiO₃ with fluoroalkylethylsilyl (FES) groups was carried out by following the procedure for partial modification of zeolite, silica, and titanium(IV) oxide (TiO₂) with alkylsilyl groups [20-26]. A schematic illustration of the procedure is shown in Scheme 1. To 0.2 g of Pt-SrTiO₃ or *p*-si/Pt-SrTiO₃, 0.03 cm³ of water was added and the mixture was stirred until the added water had been soaked into the particles. Then thus-obtained

Pt-SrTiO₃ or *p*-si/Pt-SrTiO₃ aggregates were suspended in 3 g of toluene containing 20 μmol of tridecafluoro-1.1.2.2.-tetrahydrooctyltrichlorosilane (TDFS). After shaking the mixture for 5 min at room temperature, the suspension was centrifuged and washed with toluene (ca. 5 g) and ethanol (ca. 5 g) to remove unreacted TDFS. The precipitate was then dried at 383 K overnight under evacuation. The resulting powders were labeled w/o-Pt/SrTiO₃ and w/o-*p*-si/Pt-SrTiO₃, respectively. For comparison, a Pt-SrTiO₃ powder fully covered with FES groups (*o*-Pt-SrTiO₃) was prepared without mixing water in the first step of the above-described procedure for preparation of w/o-samples.

2.4 Characterization and analytical procedures

SEM images were taken using a Hitachi S-5000 FEG scanning electron microscope at a voltage of 20 kV. Thermogravimetry-differential thermal analysis (TG-DTA) was conducted using a Bruker 2000A TG-DTA apparatus in air (flow rate: 50 cm³ min⁻¹) from room temperature to 1173 K, with a heating ramp of 10 K min⁻¹. Amounts of FES groups and silica on the surface of Pt-SrTiO₃ were determined by using a Nippon Jarrel-Ash ICPAP-575 Mark II inductively coupled plasma atomic emission spectrometer (ICP-AES). For the measurement, siliceous components on the samples were dissolved by dispersing the samples in a 0.05 mol dm³ NaOH solution for 6 h at 333 K, and the solution part was collected by centrifugal removal of remaining solid parts. Samples containing FES groups were calcined at 873 K to convert the FES groups into SiO₂ before the treatment with NaOH solution.

2.5 Photoirradiation and product analysis

The photocatalytic runs for water splitting reaction were performed in an air-free closed gas circulation system with a Pyrex reaction cell. Each sample (50 mg) was

added to 150 cm³ of water and photoirradiated in Ar. Irradiation with light of wavelength from a ultrahigh-pressure mercury arc (Ushio, 1 kW) was performed through the top of a Pyrex glass reaction vessel, so that light of wavelength longer than 290 nm reached the suspension. The temperatures of suspensions under photoirradiation were kept at 298 K in a thermostatted water bath. The amounts of H₂ and O₂ evolved were determined using a Shimadzu GC-8A gas chromatograph equipped with an MS-5A column (GL Sciences) and a TCD detector through a gas sampler (3 cm³) that was directly connected to the reaction system to prevent any contamination from air.

The apparent quantum efficiency, defined as molar ratio of the product (twice the molar amount of H₂) to the incident photons, was roughly estimated using the flux of incident photons of wavelength between 290 and 390 nm by assuming that all the photons of energy greater than their band gap (3.2 eV) were absorbed by present Pt-SrTiO₃-based photocatalysts. The incident photon flux was evaluated by total emission energy of the mercury arc at the sample position and a spectrum measured using an Ushio USR-40V/D spectra radiometer.

3. Results and Discussion

3.1 Structural characterization of Pt-SrTiO₃ covered with hollow silica

Figure 1 shows SEM images of Pt-SrTiO₃, c/SrTiO₃, si/c/SrTiO₃, and *p*-si/SrTiO₃. The Pt-SrTiO₃ samples exhibited angular morphology reflecting a cubic perovskite structure. Carbonization of glucose in the presence of Pt-SrTiO₃ produced a carbon layer on the surface of Pt-SrTiO₃: a carbon layer of ca. 20 nm in thickness entirely covers the Pt-SrTiO₃ powders (Fig. 1b). The smooth surface of c/ Pt-SrTiO₃ altered slightly to rough state after treatment of c/Pt-SrTiO₃ with APTS and TEOS (Fig. 1c).

After heat treatment of si/c/Pt-SrTiO₃ at 873 K in air, on the other hand, there was no significant change in morphology, i.e., the presence of a thin layer surrounding Pt-SrTiO₃ particles was clearly observed (Fig. 1d). From the fact that no apparent weight loss accompanied by an exothermic event was observed by TG-DTA analysis of the *p*-si/Pt-SrTiO₃ sample, complete removal of carbon components should be achieved during the heat treatment of si/c/Pt-SrTiO₃. Moreover, ICP-AES analysis for silicon indicated the presence of 2.3 wt% of silicon, corresponding to ca. 5 wt% of SiO₂, on *p*-si/Pt-SrTiO₃. These results indicate that the surface-covered layer on the *p*-si/Pt-SrTiO₃ sample consists of SiO₂, i.e., the *p*-si/Pt-SrTiO₃ particle has a core (Pt-SrTiO₃)- shell (SiO₂) structure. Another notable feature shown in the SEM images of *p*-si/SrTiO₃ is that there seems to be a void space between the core (SrTiO₃) and shell (SiO₂) where the carbon layer originally existed. The presence of a void space in *p*-si/Pt-SrTiO₃ is also supported by its relatively high BET surface area (20 m² g⁻¹) in comparison with that of the original Pt-SrTiO₃ sample (4 m² g⁻¹).

3.2 Surface characteristics of particles covered with FES groups

In order to assemble the Pt-SrTiO₃ and *p*-si/Pt-SrTiO₃ powders at the gas-water interface, it is necessary to give the particles hydrophobicity because these powders are originally hydrophilic owing to their surface hydroxyl groups. Moreover, the assembled particles should have affinity with water to induce the overall water splitting efficiently (see below). Thus, we prepared amphiphilic Pt-SrTiO₃ and *p*-si/Pt-SrTiO₃ powders (w/o-Pt-SrTiO₃ and w/o-*p*-si/Pt-SrTiO₃, respectively) by the procedure shown in Scheme 1. The strategy to make amphiphilic powders is based on aggregation of the originally hydrophilic particles by addition of a small amount of water just before the reaction with TDFS. Since the binding water between particles prevents penetration of the agent into the aggregates, FES groups can attach only on the outer parts of

aggregates. Therefore, the surfaces of the resulting powders were amphiphilic, having both hydroxyl and FES faces.

Figure 2 shows TG curves of the original Pt-SrTiO₃ and Pt-SrTiO₃ modified with FES groups measured in air in the temperature range of r.t.-1173 K. For all samples, a slight weight loss below 400 K appeared in the TG curves, probably due to dehydration and desorption of water and/or organic solvents. Moreover, samples modified with FES groups showed an additional large weight loss between ca. 500 K and ca. 800 K. Since the weight loss was accompanied by a major exothermic event starting at ca. 500 K in DTA curves of both samples (data not shown), this was ascribed to combustion of surface-grafted FES groups on w/o-Pt-SrTiO₃ and o-Pt-SrO₃. The observation of relatively large weight loss of o-Pt-SrO₃ in comparison with that of w/o-Pt-SrTiO₃ suggests relatively low surface coverage of FES groups on w/o-Pt-SrTiO₃.

For quantitative analysis of surface-loaded FES groups, amounts of FES groups on w/o-Pt-SrTiO₃ and o-Pt-SrTiO₃ were estimated by using ICP-AES analysis of silicon components. As a result, the amount of FES groups on w/o-Pt-SrTiO₃ and that on o-Pt-SrTiO₃ were determined to be 19 and 30 μmol per unit weight of the sample, respectively. From the reported cross section of an FES group (0.2 nm²) [29] and BET surface area of Pt-SrTiO₃ (4 m² g⁻¹), we calculated the surface coverage of w/o-Pt-SrTiO₃ to be ca. 60% and that of o-Pt-SrTiO₃ to be ca. 90% when monolayer coverage of FES groups was presumed. These results support the TG-DTA results described above. Thus, as has been demonstrated using monodispersed silica particles and an alkylsilylation agent [24,25], the w/o-Pt-SrTiO₃ sample prepared by the above-described procedure is likely to have an amphiphilic structure, almost half of the surface being covered with FES groups and the remainder retaining the bare hydrophilic surface. Owing to the presence of the silica shell, the amount of FES groups in the w/o-p-si/Pt-SrTiO₃ sample could not be determined. However, from the fact that almost similar weight loss originating in the combustion of FES groups was observed on the

TG-DTA measurement, this sample might also retain a hydrophilic region on the outside of the SiO₂ shell (Scheme 1).

Figure 3 shows the apparent locations of Pt-SrTiO₃ and w/o-Pt-SrTiO₃ added to water. Pictures of w/o-Pt-SrTiO₃ and w/o-*p*-si/Pt-SrTiO₃ particles after photocatalytic reaction are also shown and these are discussed below. Due to the surface hydrophilicity, the Pt-SrTiO₃ powder was preferentially dispersed in water. On the other hand, w/o-Pt-SrTiO₃ was assembled at the gas-water phase boundary, as expected. Similar behaviors were also observed when w/o-*p*-si/Pt-SrTiO₃ was used instead of w/o-Pt-SrTiO₃. These results and observations imply that w/o-Pt-SrTiO₃ and w/o-*p*-si/Pt-SrTiO₃ are assembled at the gas-water interface by facing their hydrophobic side to the gas phase and their hydrophilic side to the water phase.

3.3 Photocatalytic activity for overall water splitting on Pt-SrTiO₃ incorporated with hollow silica particles

Table 1 summarizes initial rates of H₂ and O₂ liberation on unmodified and modified Pt-SrTiO₃ powders suspended in water. Apparent quantum yields of the reaction are also shown in this Table. Similar to the results for the Pt-TiO₂ photocatalyst [18,19], stoichiometric liberation of H₂ and O₂ was observed when the suspension containing the original Pt-SrTiO₃ powder was irradiated from the top of the reaction cell (entry 1). On the other hand, the surface coverage with the carbon layer completely inhibited the H₂ and O₂ liberation: almost no H₂ and O₂ liberation was observed on c/Pt-SrTiO₃ and c/si/Pt-SrTiO₃ (entries 2 and 3). Moreover, when the *n*-si/Pt-SrTiO₃ powder, the Pt-SrTiO₃ sample directly deposited an SiO₂ layer (ca. 1wt%) on the surface, was employed, photocatalytic activity was largely suppressed (entry 4). It is likely that active sites for H₂ and O₂ production were covered with such surface components, resulting in prevention of the adsorption of water molecules on these sites.

On the other hand, despite the presence of a relatively large amount of SiO₂ on the surface in comparison with that on *n*-si/Pt-SrTiO₃, *p*-si/Pt-SrTiO₃ showed stoichiometric H₂ and O₂ liberation (entry 5). It is notable that the rate over the catalyst was comparable to that on the original Pt-SrTiO₃. This unusual photocatalytic activity is attributable to the presence of the void space, which leads to efficient contact between active sites on the Pt-SrTiO₃ surface and water.

3.4 Phase boundary photocatalytic water splitting

As depicted in Table 1, when the w/o-Pt-SrTiO₃ powder was floated and photoirradiated, the rates of H₂ and O₂ liberation became faster than those obtained on the Pt-SrTiO₃ suspension (entry 6). This result is consistent with our expectation: the backward reaction will be suppressed when the photocatalyst particles are presented at the gas-water interface. On the other hand, the o-Pt-SrTiO₃ sample, which was also floated on water, i.e., visual observation showed practically no difference from w/o-Pt-SrTiO₃, did not induce the photocatalytic water splitting efficiently (entry 7). These results indicate that the photocatalytic reaction efficiently occurred at the hydrophilic surface of w/o-Pt-SrTiO₃ facing the aqueous phase, i.e., efficient contact of the surface of photocatalyst with water is indispensable to induce the reaction. We have reported similar effects of hydrophilic surface on photocatalytic H₂ liberation from aqueous methanol solution over an amphiphilic TiO₂ photocatalyst coated with silica fine particles [26].

Figure 4 shows representative time course curves of liberation of H₂ and O₂ on w/o-Pt-SrTiO₃ floated on water. The gas phase was evacuated at 3-h intervals in this experiment. Although stoichiometric liberations of H₂ and O₂ with relatively fast rates were observed at the initial stage as mentioned above, the overall rate gradually decreased accompanied by sinking of the w/o-Pt-SrTiO₃ into water, as shown in Fig. 2c.

Since the decrease in weight loss due to combustion of surface-loaded FES groups in TG-DTA was halved on the w/o-Pt-SrTiO₃ sample after 9-h photoirradiation (data not shown), the instability was attributed to photodecomposition of FES groups on the surface through the photocatalytic reaction of Pt-SrTiO₃ [26,30].

In order to overcome the critical disadvantage of the present system, we thought that FES groups should be loaded indirectly on the surface of Pt-SrTiO₃. Thus, we employed *p*-si/Pt-SrTiO₃ particles and modified their surfaces with FES groups (w/o-*p*-si/Pt-SrTiO₃) to be assembled at the gas-water interface (Scheme 1). Figure 5 shows a typical result of photocatalytic water splitting on the w/o-*p*-si/Pt-SrTiO₃ photocatalyst. Upon photoirradiation, this photocatalyst showed constant H₂ and O₂ production for prolonged photoirradiation: the initial rates of H₂ and O₂ liberation in each run were almost constant. Moreover, the location of the particles did not change after 9-h irradiation (Fig. 2d), i.e., almost all particles were assembled at the phase boundary. Although a decrease of ca. 10% in FES groups was observed in TG-DTA probably due to the photoinduced removal of FES groups attached directly to the Pt-SrTiO₃ surface (data not shown), we confirmed that the photodecomposition was largely suppressed by the use of *p*-si/Pt-SrTiO₃.

4. Conclusions

We have developed an integrated photocatalytic system for overall water splitting using Pt-loaded photocatalytic materials. At present, the efficiency of photocatalytic reaction (0.0023, see Table 1, entry 8) is low and the reaction only occurred under ultraviolet-light irradiation because we employed commercially available SrTiO₃ powder as a bare sample. However, this system can be applied to various kinds of photocatalytic materials having high activity or having response to visible light. Studies

in these directions are now in progress.

Acknowledgements

The authors are grateful to Fuji Titanium Industry for supplying the SrTiO₃ sample. Prof. T. Hirai and Prof. Y. Shiraishi (Osaka University) are acknowledged for their help in ICP-AES measurements. This research was partially supported by a Grant-in-Aid for Young Scientists (A) (No.16685020) from the Ministry of Education, Science, Sports and Culture.

References

- [1] H. Gerischer, *J. Electroanal. Chem.* 82 (1977) 133.
- [2] M. Grätzel, *Energy Resources through, Photochemistry and Catalysis*, Academic Press, New York, 1983.
- [3] J. M. Lehn, J. P. Sauvage, R. Ziessel, *Nouv. J. Chem.* 4 (1980) 623.
- [4] A. Kudo, K. Sayama, A. Tanaka, K. Asakura, K. Domen, K. Maruya, T. Onishi, *J. Catal.* 120 (1989) 120.
- [5] H. G. Kim, D. W. Hwang, J. Kim, Y. G. Kim, J. S. Lee, *Chem. Commun.* (1999) 1077.
- [6] A. Kudo, H. Kato, S. Nakagawa, *J. Phys. Chem. B* 104 (2000) 571.
- [7] K. Domen, J. N. Kondo, M. Hara, T. Takata, *Bull. Chem. Soc. Jpn.* 73 (2000) 1307.
- [8] A. Kudo, *J. Ceram. Soc. Jpn.* 109 (2001) S81.
- [9] J. Sato, N. Saito, H. Nishiyama, Y. Inoue, *J. Phys. Chem. B* 107 (2003) 7965.

- [10] M. Machida, K. Miyazaki, S. Matsushima, M. Arai, *J. Mater. Chem.* 13 (2003) 1433.
- [11] R. Abe, M. Higashi, Z. Zou, K. Sayama, Y. Abe, H. Arakawa, *J. Phys. Chem. B* 108 (2004) 811.
- [12] J. Sato, N. Saito, Y. Yamada, K. Maeda, T. Takata, J. N. Kondo, M. Hara, H. Kobayashi, K. Domen, Y. Inoue, *J. Am. Chem. Soc.* 127 (2005) 4150.
- [13] P. Pichat, J. M. Herrmann, J. Disdier, H. Courbon, M. N. Mossanega, *Nouv. J. Chim.* 5 (1981) 627.
- [14] S.-i. Nishimoto, B. Ohtani, T. Kagiya, *J. Chem. Soc., Faraday Trans. 1* 81 (1985) 2467.
- [15] S. Ikeda, N. Sugiyama, B. Pal, G. Marci, L. Palmisano, H. Noguchi, K. Uosaki, B. Ohtani, *Phys. Chem. Chem. Phys.* 3 (2001) 267.
- [16] R. Konta, T. Ishii, H. Kato, K. Kudo, *J. Phys. Chem. B* 108 (2004) 8992.
- [17] S. Sato, J. M. White, *Chem. Phys. Lett.* 72 (1980) 83.
- [18] S. Tabata, H. Nishida, Y. Masaki, K. Tabata, *Catal. Lett.* (1995) 34.
- [19] H. Kominami, S.-y. Murakami, M. Kohno, Y. Kera, K. Okada, B. Ohtani, *Phys. Chem. Chem. Phys.* 3 (2001) 4102.
- [20] H. Nur, S. Ikeda, B. Ohtani, *Chem. Commun.* (2000) 2235.
- [21] H. Nur, S. Ikeda, B. Ohtani, *J. Catal.* 204 (2001) 402.
- [22] S. Ikeda, H. Nur, T. Sawadaishi, K. Ijiro, M. Shimomura, B. Ohtani, *Langmuir* 17 (2001) 7976.
- [23] K.-m. Choi, S. Ikeda, S. Ishino, K. Ikeue, M. Matsumura, B. Ohtani, *Appl. Catal. A* 278 (2005) 269.
- [24] Y. K. Takahara, S. Ikeda, K. Tachi, S. Ishino, K. Ikeue, T. Sakata, T. Hasegawa, H. Mori, M. Matsumura, B. Ohtani, *J. Am. Chem. Soc.* 127 (2005) 6271.
- [25] S. Ikeda, Y. K. Takahara, S. Ishino, T. Sakata, T. Hasegawa, H. Mori, M. Matsumura, B. Ohtani, *Chem. Lett.*, 34 (2005) 1386.

- [26] S. Ikeda, Y. Kowata, K. Ikeue, M. Matsumura, B. Ohtani, Appl. Catal. A 265 (2004) 69.
- [27] Japanese Patent 286728 (2001).
- [28] X. Sun, Y. Li, Angew. Chem. Int. Ed. 43 (2004) 597.
- [29] A. Fadeev, R. Helmy, S. Marcinko, Langmuir 18 (2002) 7521.
- [30] T. Kato, A. Fujishima, E. Maekawa, K. Honda, Nihon Kagaku Kaishi 1 (1986) 8.

Scheme and Figure Captions

Scheme 1. Schematic representation of the procedure for the partial loading of FES groups on Pt-SrTiO₃ and *p*-si/Pt-SrTiO₃.

Fig. 1. SEM images of (a) Pt-SrTiO₃, (b) *c*/Pt-SrTiO₃, (c) *si/c*/Pt-SrTiO₃, and (d) *p*-*si*/Pt-SrTiO₃ powders. Scale bars correspond to 300 nm.

Fig. 2. TG curves of (a) Pt-SrTiO₃, (b) *w/o*-Pt-SrTiO₃, and (c) *o*-Pt-SrTiO₃.

Fig. 3. Locations of the original Pt-SrTiO₃, *w/o*-Pt-SrTiO₃, *w/o-p*-*si*/Pt-SrTiO₃ added to water: (a) Pt-SrTiO₃, (b) *w/o*-Pt-SrTiO₃ before photoirradiation, (c) *w/o*-Pt-SrTiO₃, (d) *w/o-p*-*si*/Pt-SrTiO₃ after 9-h photoirradiation.

Fig. 4. Time course curves of H₂ (open circles) and O₂ (filled circles) liberation on *w/o*-Pt-SrTiO₃. The reaction system was evacuated at 3-h intervals.

Fig. 5. Plots of H₂ (open circles) and O₂ (filled circles) liberation on *w/o-p*-*si*/Pt-SrTiO₃ versus photoirradiation time. The reaction system was evacuated at 3-h intervals.

Table 1.Photocatalytic activity of unmodified and modified Pt-SrTiO₃ for water splitting^a

Entry	SrTiO ₃	SiO ₂ ^b (wt%)	Rate ^c (μmol h ⁻¹)		Q.E. ^d (x10 ⁻³)
			H ₂	O ₂	
1	Pt-SrTiO ₃	0	12.4	6.3	1.0
2	c/Pt-SrTiO ₃	- ^e	0	0	0
3	si/c/Pt-SrTiO ₃	- ^e	0	0	0
4	<i>n</i> -si/Pt-SrTiO ₃	1.0	2.7	0.8	0.2
5	<i>p</i> -si/Pt-SrTiO ₃	4.9	16.1	7.8	1.2
6	w/o-Pt-SrTiO ₃	- ^e	17.9	9.2	1.4
7	o-Pt-SrTiO ₃	- ^e	4.1	1.6	0.3
8	w/o- <i>p</i> -si/Pt-SrTiO ₃	- ^e	28.7	13.6	2.3

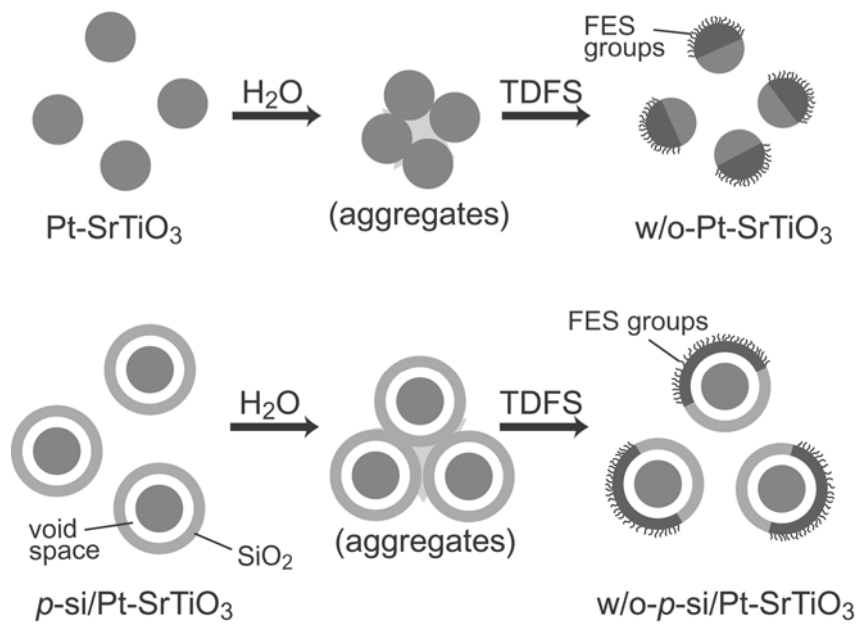
^a Catalyst (50 mg) and pure water (150 cm³) were added to a reaction cell and were photoirradiated from the top part of the cell under Ar (5 kPa).

^b Content of SiO₂ on the sample determined by ICP-AES.

^c Initial rate for 1 h.

^d Apparent quantum efficiency estimated by the initial rate of H₂ liberation and the flux of incident photons of wavelength between 290 and 390 nm.

^e Not measured.



Scheme 1

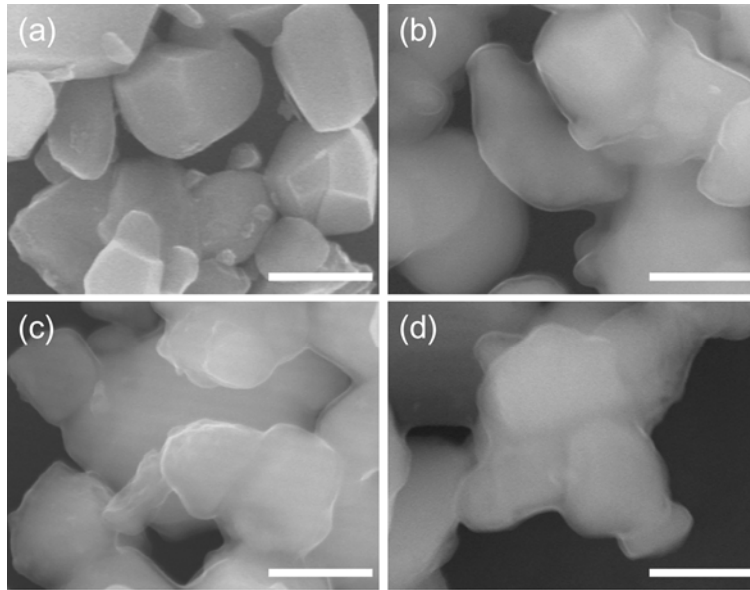


Figure 1

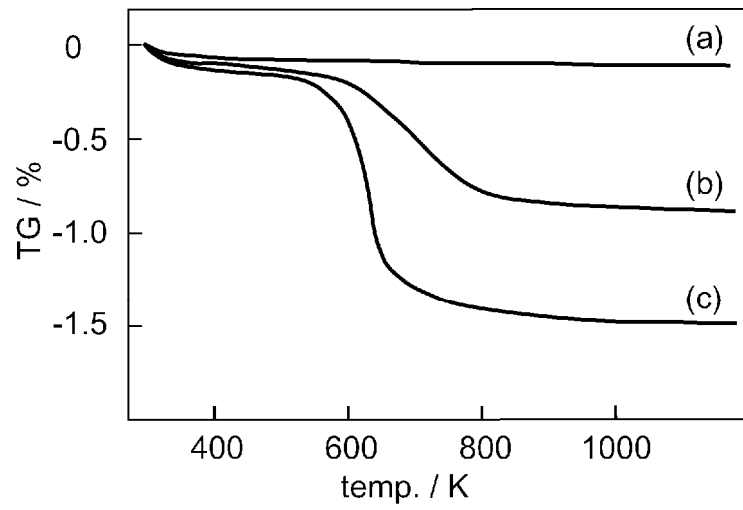


Figure 2

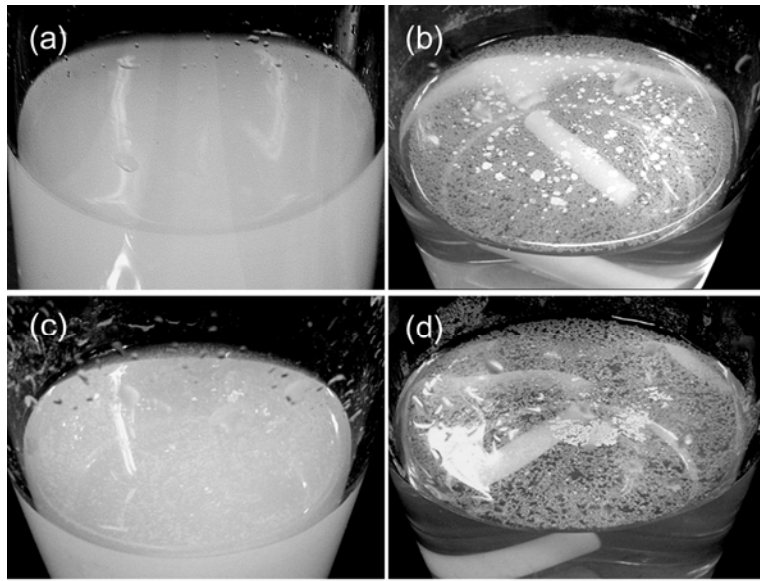


Figure 3

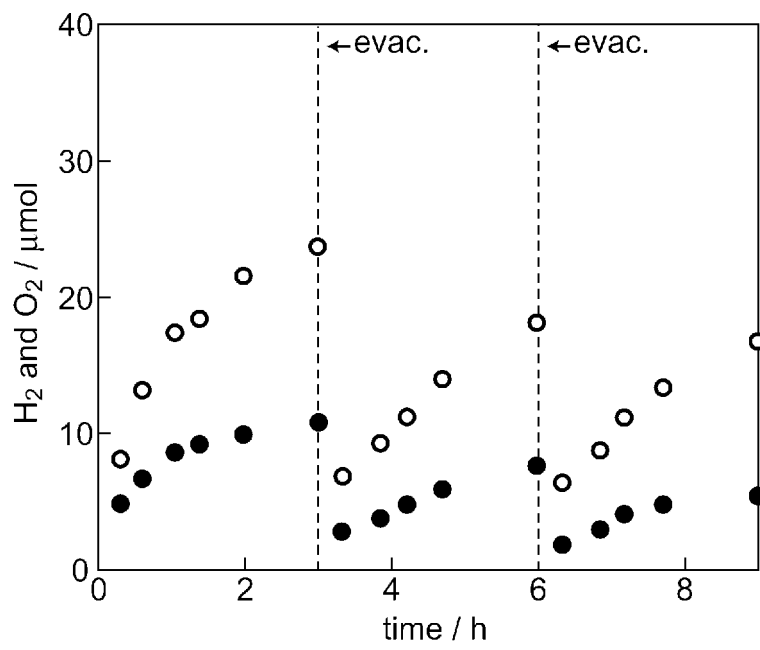


Figure 4

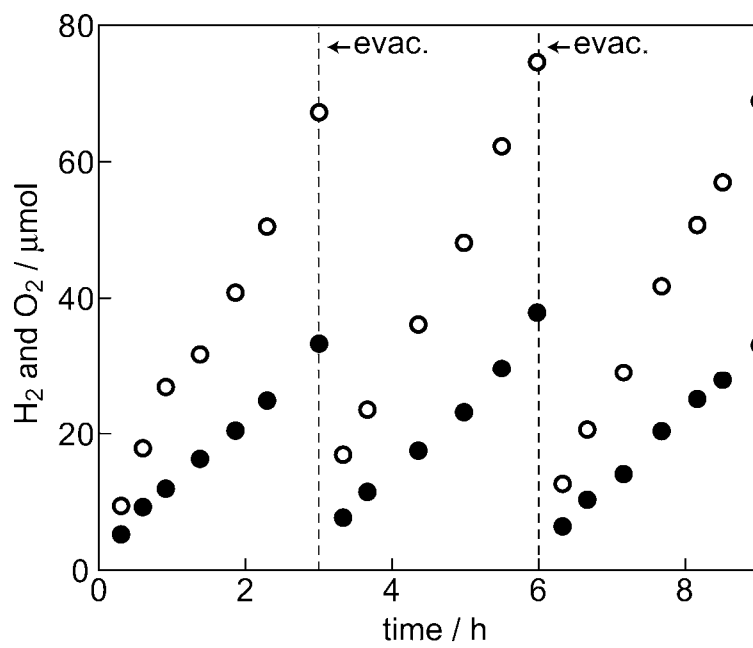


Figure 5